# On Divergence in Radiation Fields

Joerg Fricke
Dept. of Mechanical Engineering
University of Applied Sciences Muenster
Muenster, NRW, Germany
j.fricke@bkbmail.de

#### ABSTRACT

Three thought experiments demonstrate that under certain circumstances radiation fields have to be attenuated or amplified multiplicatively in order not to violate the conservation of energy. Modulation of radiation by means other than superposition is theoretically made possible by plugging additional terms into the source slots of the Maxwell equations. Modulated radiation would enable the well focused stimulation of neurons for diagnostic and therapeutic purposes.

### I. Introduction

The Maxwell equations describe basic relationships whose validity within the domain of classical electromagnetism is beyond doubt after successful application for one and a half century. However, there are reasons to believe that the question is still not settled which quantities have to be plugged into the "source slots" offered by the equations, starting, as far as I know, with Heaviside's duplex equations. The modern point of view is that charges and currents of charges are inherently coupled to particles, and that they are the sources of fields. But there were attempts to introduce (sometimes implicitly) some kind of "particle-free" field divergence which is not the cause but an effect of the field [1]. For the most general case, the duplex equations could be enhanced to read

$$\nabla \times \mathbf{E} = -\frac{\partial \mathbf{B}}{\partial t} - \rho_m \mathbf{u_m} - \varsigma_m \mathbf{v_m}$$
 (1)

$$\nabla \times \mathbf{H} = \frac{\partial \mathbf{D}}{\partial t} + \rho_e \ \mathbf{u}_e + \varsigma_e \ \mathbf{v}_e$$
 (2)

with  $\rho_e$  and  $\rho_m$  denoting the particle-bound densities of the divergence of  $\mathbf{D}$  resp.  $\mathbf{B}$ ,  $\boldsymbol{\varsigma}_e$  and  $\boldsymbol{\varsigma}_m$  standing for the particle-free densities of the divergence of  $\mathbf{D}$  resp.  $\mathbf{B}$ ,  $\mathbf{u}_e$  and  $\mathbf{u}_m$  representing the velocities of the particles contributing to  $\rho_e$  resp.  $\rho_m$ , and  $\mathbf{v}_e$  and  $\mathbf{v}_m$  being virtual velocities assigned to  $\boldsymbol{\varsigma}_e$  resp.  $\boldsymbol{\varsigma}_m$ . Usually, the current density  $\mathbf{J}_e = \rho_e \, \mathbf{u}_e$  is introduced, and accordingly one could define the current densities  $\mathbf{J}_m = \rho_m \, \mathbf{u}_m$ ,  $\mathbf{J}_{\varsigma e} = \boldsymbol{\varsigma}_e \, \mathbf{v}_e$ , and  $\mathbf{J}_{\varsigma m} = \boldsymbol{\varsigma}_m \, \mathbf{v}_m$ . Of course, according to the state of the art,  $\boldsymbol{\rho}_m = 0$ ,  $\mathbf{J}_m = \mathbf{0}$ , and

$$\boldsymbol{\varsigma}_e = 0$$
 (3a)  $\boldsymbol{J}_{ce} = \boldsymbol{\varsigma}_e \ \boldsymbol{v}_e = \boldsymbol{0}$  (3b)

$$\boldsymbol{\varsigma}_{m} = 0 \qquad (4a) \qquad \boldsymbol{J}_{cm} = \boldsymbol{\varsigma}_{m} \, \boldsymbol{v}_{m} = \boldsymbol{0} \qquad (4b)$$

As a consequence of Eq. 3 and 4, fields cannot be attenuated multiplicatively but by superposition only. This is certainly true for static fields. As an illustration for radiation fields,

consider two separated volumes of space  $V_0$  and  $V_1$  surrounded by vacuum, each containing a known distribution of charges and currents causing the fields  $R_0$  resp.  $R_1$ . Assume that  $R_0$  in the absence of the sources in  $V_1$  is already known. It is legitimate to calculate the net field by first calculating  $R_1$ , taking into account the sources inside  $V_1$  only, and then determining the net field by adding  $R_0$  and  $R_1$ . Both  $R_0$  and  $R_1$  comply with the Maxwell equations, and so does the net field, of course. Eq. 3 and 4 hold if the power exchanged between  $R_0$  and the sources in  $V_1$ , and between  $R_1$  and the sources in  $V_0$  is exactly balanced by interference of  $R_0$  and  $R_1$ . This is usually the case but the subject of this paper is the demonstration of counter-examples.

A seeming exception is the concept of "penetration depth". If  $V_1$  would contain only a thick sheet of metal, one could multiply  $R_0$  inside the metal with a term  $\exp(-s/\delta)$  where s denotes the distance from the surface and  $\delta$  the penetration depth, calculate the loss, and limit  $R_1$  to the reflected wave. While this procedure yields the measurable quantities correctly, each field component in itself does not comply with the Maxwell equations if Eq. 3 and 4 hold. A rigorous treatment has to be based on the extinction theorem [2].

The application of Eq. 3 and 4 to radiation fields is reasonable but not based on direct experimental data [3]. Actually, a direct measurement of the divergence of a radiation field does not seem to be feasable. The aim of this paper is to provide three counter-examples to Eq. 3 and 4 in form of thought experiments. The rest of the paper is organized as follows: In the second section, assumptions and characteristics of the systems employed in the thought experiments are delineated. The third section describes the experiments itself, while the fourth outlines the immediate consequence for the theory and a way of experimental verification. The appendix provides the details of the calculations done in the framework of the first and second thought experiment.

#### II. METHOD

The direct method of testing the general validity of Eq. 3 and 4 were to consider a charged particle moving in a radiation field as fundamental as possible. The energy spent by the radiation source has to equal the sum of the energies absorbed by the charge and radiated to infinity [4]. However, this method turns out to be difficult for several reasons:

- It seems to be impossible to solve the problem in a symbolical way; therefore one has to resort to numerical calculations.
- Generally, the phase relation between the incident field and the field scattered from a point charge on a closed surface at a large distance from the particle is a highly oscillatory function of position. Therefore, numerically integrating the power flow through such a surface is error prone resp. computationally costly.
- Arbitrary fields can be calculated by integrating over an angular spectrum of plane waves. So, inhomogeneous plane waves can be considered to be among the most elementary components of fields, with uniform plane waves being a limiting case. However, there can be no pure inhomogeneous wave without any material boundary. It follows that the treatment has to take into account the interaction of charged particle and boundary.

The second and third difficulty does not occur if the point charge is replaced by a nonradiating system. It is well known that if Eq. 3 and 4 hold a nonradiating system cannot absorb energy from

radiation fields. So, in order to disprove the general validity of Eq. 3 and 4 it is sufficient to demonstrate a nonradiating system absorbing energy. Obviously, this is a case where dealing with a system is easier than treating its components separately.

The only requirement for a thought experiment is that it does not violate any laws of physics. Technical feasibility or the probability of occurrence of the situation under consideration in a "natural" context are inessential. The following features greatly facilitate the calculations without introducing any basic impossibilities:

- Each (macroscopic) component of the system moves on predetermined paths not influenced by
  the incident radiation field. Every detail of the incident field is known in advance, so this
  feature could be achieved by exchange of energy and momentum with a remote system without
  any feedback. For example, the frequency of the incident field could be located in the
  microwave domain while the exchange is carried out via visible light.
- The system does not scatter the incident field but is completely transparent. This could be accomplished by dividing the system into electrically small parts which are coupled by controlled current sources, i. e. the system is composed of an active controlled metamaterial. As above, no feedback mechanism is required because the incident field is known in advance.
- All actions, whether mechanical or electrical, are performed with an efficiency of 1.

The first feature has two consequences: Regardless of the force exerted by the incident field, the center of the nonradiating system can move with constant velocity, avoiding difficulties related to mass or self-force which could be encountered when dealing with accelerated particles at relativistic speed. If the incident field loses or gains energy, the difference of this energy and the growth or loss of internal energy (e. g. internal stress) is transferred via the nonradiating system ultimately to or from the remote system.

#### III. THOUGHT EXPERIMENTS

## A. Spherical Shell with Constant Radius in an Inhomogeneous Field

The magnitude of the phase velocity  $\mathbf{u}_{\mathbf{p}}$  of inhomogeneous plane waves is less than the speed of light; so, in principle, any material object can move with such a field in a phase-locked way. Here a monochromatic field is employed.

In this first thought experiment, a nonconducting, evenly charged spherical shell maintains a constant radius. At its center, a point charge is located of opposite polarity but same amount as compared to the charge on the shell. Consequently, there is no field outside the shell. The shell moves uniformly with a speed  $u_s$  not much less than the speed of light, e. g.  $u_s = 0.9 c$  which yields  $\gamma = 1 / \sqrt{1 - u_s^2 / c^2} \approx 2.29$ . So, seen from the laboratory rest frame (LRF), the shell is distinctly spheroidal. In Cartesian coordinates, the center of the shell moves parallel to the z-axis toward positive z-values.

With reference to Cartesian coordinates  $x_f$ ,  $y_f$ , and  $z_f$ , the field propagates toward positive  $z_f$ -values, has an exponentially decreasing amplitude in the direction of the positive  $x_f$ -axis, and consists of the transversal components  $E_T = E_{x_f}$  and  $B_{y_f}$ , and the longitudinal component  $E_L = E_{z_f}$ .

Figure 1 shows a cross-section of the upward moving shell, its velocity  $\mathbf{u}_s$  forming the angle  $\alpha$  with the phase velocity  $\mathbf{u}_p$  of the field. The gray arrows represent the field components  $E_L$  and

 $E_T$ . At the thin oblique lines parallel to the  $x_f$ -axis,  $E_T = 0$ , and  $|E_L|$  is at its maximum. The decreasing amplitude is indicated by the two  $E_T$  arrows of different lengths.  $F_C$  is the force exerted on the center charge by  $E_L$ ,  $F_L$  and  $F_T$  are exerted on the shell by  $E_L$  resp. by  $E_T$ .  $F_C$  and  $F_L$  are not shown in Fig. 1.

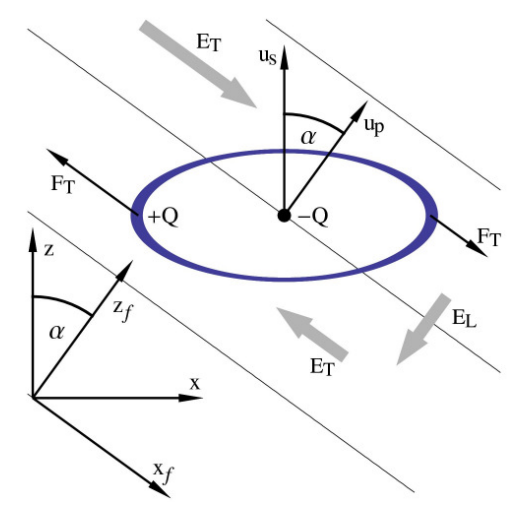


Fig. 1 Cross-section of shell, velocities, electric field components, and force

With  $\alpha=0$ ,  $F_C+F_L=0$  independently of the phase of  $E_L$  at the location of the center charge, as expected. If the center is placed at a point where  $E_T=0$  as in Fig. 1,  $F_T=0$  because the shell is immersed symmetrically into two  $E_T$ -half-waves of different direction. With the center placed at  $E_T=0$ , the  $E_L$  component forms a saddle surface at the place of the shell, and  $\alpha=0$  results in the maximum force  $F_L$  exerted on the charged spheroid.

When  $\alpha$  increases, the extend of the shell along the  $x_f$ -axis decreases, thereby decreasing  $F_L$ , and the extend along the  $z_f$ -axis increases, decreasing  $F_L$  further. The shell is now located in two  $E_T$ -half-waves of different mean strength. For the case  $\alpha = \pi/5$ , the components of  $F_T$  are therefore depicted in Fig. 1 by arrows of different lengths.

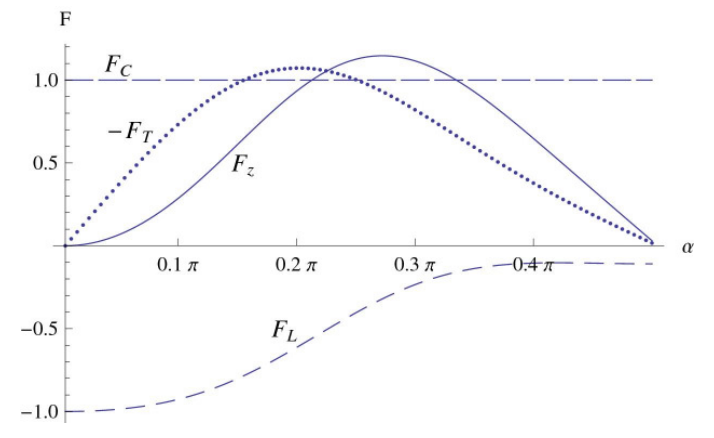


Fig. 2 Forces exerted on the charge as a function of  $\alpha$ 

Figure 2 shows the dependence of the forces on the angle  $\alpha$ . For each value of  $\alpha$ ,  $u_P$  was adjusted to yield a phase-locked movement of the shell, the radius of the shell was set to  $\lambda/2$ , and the field strength was adjusted to result in  $F_C = 1$ .  $F_L$  and  $-F_T$  are shown as computed parallel to the  $z_f$ -axis resp. antiparallel to the  $x_f$ -axis. The z-component  $F_z = (F_C + F_L) \cos \alpha - F_T \sin \alpha$  of the total force  $\mathbf{F}_{tot}$  raises even above  $F_C$  for  $\alpha$  in the range  $\pi/4$  to  $\pi/3$ .

Because  $\mathbf{F}_{tot} \cdot \mathbf{u}_s > 0$  for  $0 < \alpha < \pi/2$ , there is obviously an energy transfer from the incident field to the nonradiating system. The flow of energy from the incident field to the shell as expressed by the Poynting vector is limited to the inside of the shell. From a classical point of view, the system could only absorb the field energy which is currently available inside the shell. In a real experiment, the shell were bound to collide with the material boundary along which the field is propagating after a short time interval, of course.

Beside the force exerted by the external field on the moving shell, there are two other sources or sinks of energy: The growing mechanical stress of the shell and the energy difference created by the superposition of the external and internal fields while the strength of the external field increases. To prove that nevertheless a transfer of energy to or from the remote system takes places, at least three ways can be taken:

• For a given polarity of the charges of the nonradiating system, both the direction of the forces and the sign of the energy difference due to superposition depend on the polarity of the half wave at the point charge but the amount of stress does not. From the assumption that independent of the polarity of the half wave there is no energy transfer to the remote system:  $W_F + W_{Su} + W_{St} = 0 = -(W_F + W_{Su}) + W_{St}$  follows

$$W_F + W_{Su} = -(W_F + W_{Su}) = -W_{St}$$
 (5)

with the energy  $W_F$  associated with the force exerted by the external field, the energy difference  $W_{Su}$  caused by superposition, and the energy  $W_{St}$  associated with the mechanical stress. However, Eq. 5 can be true only if  $W_{St} = 0$  which is certainly not the case.

- The point charge can be replaced by a second charged shell with a diameter less than that of the first one. The diameter of both concentric shells can be varied without causing radiation (as discussed in section B below in more detail). If both diameters are the same at the start and at the end of the observation period then the energy difference  $W_{Su}$  is zero at the beginning and at the end. However, the force caused by the B component of the external field is not zero while the diameters are changing. In order to avoid compensation of the forces exerted by the E component and by the B component, the speed of the shells has to differ slightly from the phase velocity of the plane wave. Then the timing in relation to the phase of the external field can be chosen in such a way that, for example, the integral of the B force over time vanishes but the integral of the E force over time does not.
- Instead of letting the charge of the nonradiating system vanish at the beginning and the end of the observation period, one can consider a spatially limited radiation field such as a beam. This is the subject of the following section.

## B. Shell with Variable Radius in a Radially Polarized Beam

The motivation to investigate the effect of an inhomogeneous field on a charged shell sprang from a similar approach using a beam. With this earlier setup, the effect cannot be easily visualized because the field components of a beam near the focus are more complicated than a

plane field, the force caused by the *B* component cannot be neglected because the radius of the shell varies, and the magnitude of the effect is small. Nevertheless it is included here in order to show that nonradiating absorption is not limited to evanescent waves.

As in the first thought experiment, the absorbing system is a nonconducting, evenly charged spherical shell. Seen from the rest frame of the center of the shell (SRF), it does not radiate if it oscillates radially with an arbitrary frequency spectrum and with both amplitude and phase independent of the angle. Since the power radiated by a charge is the same in all inertial frames the shell remains nonradiating as long as its center moves without acceleration. The mechanism maintaining the oscillation has to overcome the self-force of the charge. After the radius has returned to its initial value the total energy spent is zero, because there is no radiation loss.

Incident radiation fields do not contribute to the energy turnover of the oscillation: Seen from the SRF, the charge is moving exclusively radially in the B component of any external field resulting in the spent power  $P_{BR}(t) = 0$ . The power  $P_{ER}(t)$  exchanged between the E component and the charge Q on the shell S is given by

$$P_{ER}(t) = \iint_{S} \sigma_{q}(t) \mathbf{E}(\mathbf{r}, t) \cdot \mathbf{v}_{\mathbf{R}}(t) dS = Q \mathbf{v}_{\mathbf{R}}(t) \cdot \hat{\mathbf{n}} \iint_{S} \mathbf{E}(\mathbf{r}, t) \cdot \hat{\mathbf{n}} dS = 0$$
 (6)

because  $\iint_{S} \mathbf{E}(\mathbf{r},t) \cdot \hat{\mathbf{n}} dS = 0$  for the incident field  $\mathbf{E}(\mathbf{r},t)$ , with charge density  $\sigma_q(t)$ , radial

velocity  $\mathbf{v}_{R}(t)$ , differential shell area dS, and unit vector  $\hat{\mathbf{n}}$  normal to dS. So, the total power exchanged between the incident field and the mechanism driving the oscillation is  $P_{R}(t) = P_{BR}(t) + P_{ER}(t) = 0$  in every moment. Since the amount of energy spent or gained by a system does not depend on the frame of reference,  $P_{R}(t) = 0$  in every inertial frame. However, seen from frames other than SRF a translational movement of the charge is added, and amplitude and phase of the radial velocity depend on location, due to relativistic effects. Generally, only  $P_{ER}(t) = -P_{BR}(t)$  holds.

In the present case, the elimination of the field outside the shell by a center charge is not necessary because the source of the beam can be located so distantly that the quasi-static field of the shell has no effect on it. The shell traverses the focus perpendicular to the axis of the beam; its radius increases and decreases once while passing through the focus; please see the equation for  $R'_{\nu}(t')$  in the appendix.

Calculations were performed with a beam of frequency  $f=3\,\mathrm{GHz}$  and  $k\,w_0=1.3\pi$ , and the shell parameters  $R_0=0.1\lambda$ ,  $u_S=0.9\,c$ ,  $\tau=1/(2\,\omega)$ ,  $t_0=T/\gamma$ , and  $t_1=0$ ,  $\lambda$ ,  $\omega$ , and T being the wavelength, the angular frequency resp. the period of the beam. The mean force acting on the shell while completely traversing the beam vanishes if  $A_S=0$  (constant radius), as expected, but it does not vanish if  $A_S=0.1\lambda$ . A series of shells with thus varying radius crossing the focus with the same frequency as the beam, each shell carrying a charge of 1 nC, equivalent to a current of 3A, results in a power exchange between the beam and the remote system via the shells of about 400 ppm of the beam's power.

This second thought experiment demonstrates an additional aspect which was perhaps not obvious in the first experiment: While the conservation of energy would be satisfied by a slight attenuation or amplification of the beam behind the focus, the conservation of momentum requires a minor deflection of the beam.

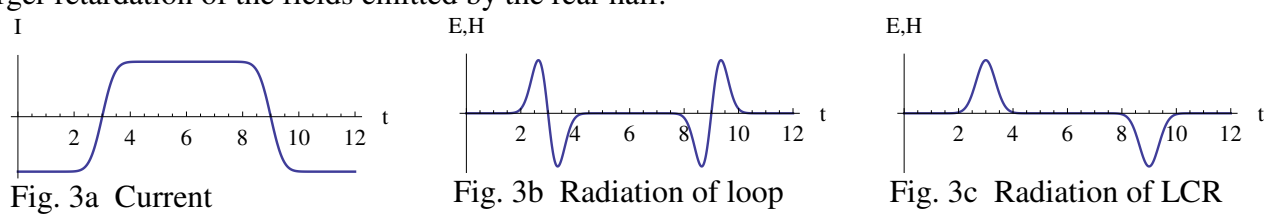
# C. Effect of a modulator carrying a DC current on a UWB field

As discussed in the introduction, the results of the thought experiments described above suggest that particle-free divergence, of the E component as well as of the H component of radiation, is necessary. Associated with the divergences  $\varsigma_e$  and  $\varsigma_m$  are the current densities  $\mathbf{J}_{\varsigma_m}$  and  $\mathbf{J}_{\varsigma_m}$ . Since both the current density  $\mathbf{J}_{\rho m}$  of magnetic monopoles and the current density  $\mathbf{J}_{\varsigma_m}$  of particle-free divergence contribute to the curl of the E field, one is naturally reminded of the setups dedicated to the verification of the existence of magnetic monopoles. Some of these are based on the fact that a single magnetic monopole would constitute a magnetic current with a DC component, and as a consequence the associated curl of E would show a DC component, too. The goal of the third thought experiment is to accomplish a curl of E with a DC component.

While the third thought experiment avoids macroscopic bodies which move almost with the speed of light, at the outset it is based on two other unrealistic assumptions for the sake of simplicity: The existence of an abundance of magnetic monopoles, and a system of infinite length. However in section IV, it will be shown that both assumptions are not crucial to the function of the system.

Provided that there is an abundance of magnetic monopoles under certain conditions, it should be possible to build some kind of magnetic current sources and to guide currents by "magnetic conductors". Again for the sake of simplicity, the electric and magnetic current sources used in the following setup are supposed to fit into a cylinder whose length and diameter is not considerably larger than the diameter of the adjacent conductors.

Consider a circular loop made out of controlled electric current sources connected by pieces of electrically conducting wire. The sources deliver synchronously a periodic current as depicted in Fig. 3a, and the wires are electrically short, in terms of the duration of the current ramps. It is well known that the radiation of the loop develops like Fig. 3b, with details depending on the radius of the loop. In a formal way, this can be explained by treating the loop as a magnetic dipole or, in the case of large loops as a multitude of adjacent dipoles. Generally, the radiation of a dipole depends on the second time derivative of the dipole moment or, in the case of magnetic dipoles, of the current constituting the dipole. Another point of view is that the fields caused by the front half and by the rear half of the loop are of opposite polarity but do not exactly cancel each other due to the larger retardation of the fields emitted by the rear half.



In a certain class of current loops called "large current radiators" (LCR), the effect of the rear half of the loop is largely suppressed by shielding; this is achieved either by separating the front half and the rear half by a sheet of material [5] or by designing the front half itself as a shield [6]. In a schematic way, Fig. 3c shows the resulting radiation fields in that volume of space where the shielding is effective. The similarity of LCRs to electric dipoles is that the strength of the radiation is proportional to the first time derivative of the current; the difference is that the time intervals between current ramps and hence between consecutive unipolar radiation pulses are not limited by the accumulation of charge. A limitation is only given by the ratio of the penetration depth at the fundamental frequency of the current to the actual thickness of the layer of shielding material.

A considerable shielding effect is accomplished by inserting a cylinder of dissipative material coaxially into the loop. Following a suggestion by Harmuth, at least the outer layer of the cylinder should consist of a ferrite material in order to have reflections with inverted H field instead of inverted E field. (Since the H field of the backward radiation is already inverted compared to the forward radiation, the polarity of the radiation reflected by ferrite is identical to that of the forward radiation.) In cylindrical coordinates  $(\rho, \varphi, z)$ , with the axes of the loop and of the cylinder identical to the z-axis, this yields an LCR whose radiation fields are independent of  $\varphi$ .

In the next step, we replace the current loop by a multitude of loops of identical diameter, all coaxial to the z-axis, being evenly distributed along the z-axis, carrying synchronous currents, and sharing a dissipative cylinder D. For the sake of simplicity, let the length  $L_R$  of this radiating coil R and of the cylinder D approach infinity. Outside the coil R, the quasistatic component  $H_R$  of its field virtually vanishes. As depicted in Fig. 4, the trailing edge of each radiation pulse is flattened due to the spatial distribution of sources. However, the amounts of energy of successive pulses are still well separated.



The radiator R is coaxially enclosed by a modulator M and by an absorber A, both in the form of an open cylinder. Fig. 5 shows a cross-section of a 30° sector; the whole setup is circular, of course. The modulator M is made out of short pieces of magnetic conductors connecting sources of a constant magnetic current  $I_{Mz}$  which flows parallel to the z-axis. Due to symmetry. the static field  $\mathbf{E}_{\mathbf{M}}$  of the modulator is zero on the inside of M, and contains only a  $\varphi$ -component  $E_{M\varphi}$  on the outside.

As implied in Fig. 5, the space between R and M contains neither static nor quasistatic fields but is only traversed by the radiation pulses RI. As a consequence, the energy flow associated with a radiation pulse is not altered by the modulator as long as the pulse is inside the modulator. While a pulse comprised of the field components  $E_{R\phi}$  and  $H_{Rz}$  passes the modulator there is an exchange of energy between the pulse and the magnetic current sources. If  $H_{Rz}$  and  $I_{Mz}$  are paral-

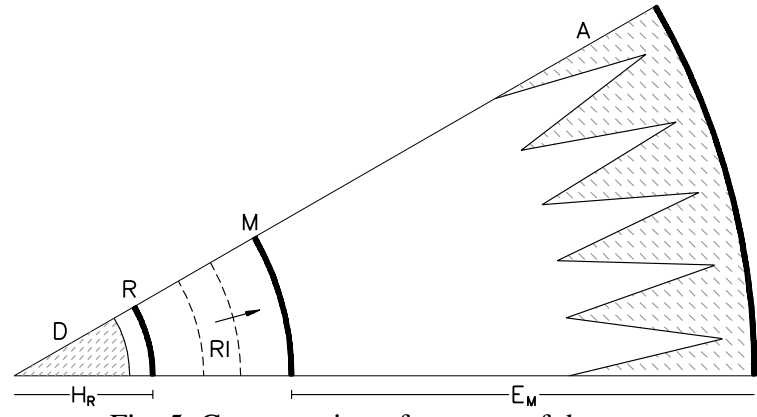


Fig. 5 Cross-section of a sector of the setup

lel energy flows from the radiation to the sources, if antiparallel the sources deliver energy to the radiation. Outside the modulator, the change of energy carried by the pulse is accounted for by the superposition of  $E_{M\varphi}$  and  $E_{R\varphi}$ : The amount of power flow density is now  $S_{\rho} = (E_{M\varphi} + E_{R\varphi}) \cdot H_{Rz}$ .

Due to geometry, with increasing distance r from the z-axis both  $E_{M\phi}$  and  $S_{\rho}$  have to decrease proportionally to 1/r; consequently, in the absence of the modulator both  $E_{R\phi}$  and  $H_{Rz}$  would decrease proportionally to  $1/\sqrt{r}$ . With the modulator in place, the fields are expected to remain unaltered by superposition. However, since  $E_{M\phi}$  decreases faster than  $E_{R\phi}$  and  $H_{Rz}$  the radiation would regain the power flow it had without passing the magnetic current sheet. But this would violate the principle of conservation of energy. So, while propagating away from the modulator the field components of the radiation have to be deflated or inflated, depending on the polarity of the pulse.

Contrary to the other thought experiments, the total amount of energy transferred between radiation and modulator is zero. The scheme of this third experiment would not work with CW radiation because its energy is not localized in single half waves. But if a UWB radiation pulse is generated only after a considerable amount of energy of its predecessor has been absorbed by the absorber A, the deflation or inflation of the radiation fields cannot be prevented by energy exchange between successive pulses. Because pulses of one polarity are deflated and those of the other polarity inflated the direction of the associated current density  $\mathbf{J}_{\varsigma m}$  is the same for pulses of both polarities. As mentioned at the outset of section C, a current density with a DC component is expected to be accompanied by a curl of the E field with a DC component, too.

Due to the well known duality of the E field and the H field as well as of the electric charge and the (hypothetical) magnetic charge, the result of this thought experiment remains basically the same if a magnetic current flows in the radiator R and an electric current in the modulator M.

### IV. DISCUSSION

*Immediate Impact on the Theory* 

All three thought experiments result in a paradox: In the first and the second, while the incident fields exert a force parallel to the velocity of the shell and therefore transfer energy and momentum via the shell to the remote system, Eq. 3 and 4 force the incident fields to continue unchanged in the absence of a secondary field emitted by the shell. In the third, the radiation pulses first exchange energy with the modulator, and during further propagation regain the energy they had before passing the modulator. Deflating fields would lose energy and momentum, inflating fields would gain both, so no conservation law would be violated. In order to enable the deflation or inflation of radiation fields, the densities of particle-free divergence  $\varsigma_e$  and  $\varsigma_m$  have to be nonzero. The virtual velocities  $\mathbf{v}_e$  and  $\mathbf{v}_m$  used in Eq. 1 and 2 can be determined by using these same equations. Setting the terms  $\rho_e$   $\mathbf{u}_e$  and  $\rho_m$   $\mathbf{u}_m$  to zero, and replacing  $\varsigma_e$  and  $\varsigma_m$  by  $\nabla \cdot \mathbf{D}$  resp.  $\nabla \cdot \mathbf{B}$  results in

$$\mathbf{v}_{\mathbf{e}} = (\nabla \times \mathbf{H} - \partial \mathbf{D} / \partial t) / \nabla \cdot \mathbf{D} \tag{7}$$

$$\mathbf{v}_{\mathbf{m}} = -(\nabla \times \mathbf{E} + \partial \mathbf{B} / \partial t) / \nabla \cdot \mathbf{B}$$
 (8)

Magnitude and direction of  $\mathbf{v_e}$  and  $\mathbf{v_m}$  depend on the orientation of the gradient of attenuation relative to both the direction of propagation and the orientation of  $\mathbf{E}$  resp.  $\mathbf{H}$ . As an example, consider a homogeneous plane wave consisting of an  $E_x$ -component and a  $H_y$ -component, propagating parallel to the z-axis toward positive z-values. A gradient of attenuation independent of location, and given by the elevation angle  $\vartheta$  and the azimuthal angle  $\varphi$  results in

$$\mathbf{v}_{\mathbf{e}} = -c \cot \vartheta \sec \varphi \, \mathbf{e}_{\mathbf{v}} + 0 \, \mathbf{e}_{\mathbf{v}} + c \, \mathbf{e}_{\mathbf{v}}$$
 (9)

$$\mathbf{v}_{\mathbf{m}} = 0 \, \mathbf{e}_{\mathbf{x}} - c \, \cot \vartheta \, \csc \varphi \, \mathbf{e}_{\mathbf{v}} + c \, \mathbf{e}_{\mathbf{z}} \tag{10}$$

with the standard basis vectors  $\mathbf{e}_{\mathbf{x}}$ ,  $\mathbf{e}_{\mathbf{y}}$ , and  $\mathbf{e}_{\mathbf{z}}$ . Obviously,  $c \leq |\mathbf{v}_{\mathbf{e}}| \leq \infty$  and  $c \leq |\mathbf{v}_{\mathbf{m}}| \leq \infty$ . This poses no problem because these virtual velocities are not associated with the motion of matter or energy. Put in a pictorial way, if Faraday's "lines of force" would propagate with the radiation field,  $\varsigma_e \neq 0$  and  $\varsigma_m \neq 0$  would indicate that some of these lines have "open ends", with  $\mathbf{v}_{\mathbf{e}}$  and  $\mathbf{v}_{\mathbf{m}}$  describing the movement of these open ends.

With the current densities  $\mathbf{J}_{\rho e} = \rho_e \, \mathbf{u}_e$ ,  $\mathbf{J}_{\varsigma e} = \varsigma_e \, \mathbf{v}_e$ ,  $\mathbf{J}_{\varsigma m} = \varsigma_m \, \mathbf{v}_m$ , and  $\rho_m = 0$  confirming the absence of magnetic monopoles, the Maxwell equations in the usual redundant form read

$$\nabla \times \mathbf{E} = -\partial \mathbf{B} / \partial t - \mathbf{J}_{cm} \tag{11}$$

$$\nabla \times \mathbf{H} = \partial \mathbf{D} / \partial t + \mathbf{J}_{\rho e} + \mathbf{J}_{ce}$$
 (12)

$$\nabla \cdot \mathbf{D} = \rho_e + \zeta_e \tag{13}$$

$$\nabla \cdot \mathbf{B} = \zeta_m \tag{14}$$

supplemented by the continuity equations  $\nabla \cdot \mathbf{J}_{\rho e} = -\partial \rho_e / \partial t$ ,  $\nabla \cdot \mathbf{J}_{\varsigma e} = -\partial \varsigma_e / \partial t$ , and  $\nabla \cdot \mathbf{J}_{\varsigma m} = -\partial \varsigma_m / \partial t$ .

## Verification and Application

Of course, the enhanced Maxwell equations have to be supplemented by further modifications of the theory, and several questions have to be answered, first of all, if and how the existence of "deflating" or "inflating" radiation fields could be proved or disproved experimentally.

In the framework of the current technology, it is not possible to implement the first two thought experiments in reality. However, since the total effect of a set of charges is the linear superposition of the effects of all the single charges involved, one could determine a small subset of charges whose effect is maximal, and replace these charges by current pulses on some kind of "one-dimensional active metamaterial". Modulating a sequence of current pulses using a low frequency, and in turn modulating monochromatic radiation by these pulses would result in easily detectable sidebands which could not be generated by superposition.

But with two modifications, the third thought experiment seems to provide the easiest implementation: First, the length of the setup has to be reduced from infinity to a size fitting in common laboratories. This can be achieved by terminating the ends of the radiator and of the modulator by horizontal disks which form parallel plates guiding the radiation. Behind the absorber A these disks can be connected by an open cylinder. Thus, the dissipative cylinder inside the radiator R, the disks, and the cylinder behind the absorber A form a kind of pot core. With an

electric radiator and a magnetic modulator, this pot core has to be made from ferrite material, with a magnetic radiator and an electric modulator the pot core has to be metallic. Since in the microwave domain ferrite is quite dissipative, a metallic pot core is preferable, and so is a setup containing a magnetic radiator and an electric modulator.

Second, the magnetic monopole current has to be replaced by magnetic dipoles changing their orientation [7]. So, a constant magnetic current can be achieved only in limited time intervals by coils carrying a current whose first time derivative is constant during these intervals. A magnetic radiator can be operated like its electric counterpart, generating radiation while the first time derivative of the current changes its sign. The toroidal coils replacing the current loops have to be "transparent", i. e. the loops forming the toroids may not have LCR behavior but that of unshielded loops with radiation depending on the second time derivative of the current.

Upon confirmation by experiments, the question of applications would rise. By multiplicatively attenuating radiation fields, it will be possible to generate low frequency components in UWB fields. That will enable the stimulation of neurons for diagnostic and therapeutic purposes, using UWB fields focused to a smaller volume than is possible by employing near fields as is the state of the art.

## APPENDIX: EQUATIONS USED IN THE CALCULATIONS

Two rest frames are used, one defined by a fictitious laboratory (LRF) which is identical to the rest frame of the focus in the second thought experiment, the other by the center of the spherical shell (SRF). Quantities as seen from SRF are indicated by an apostrophe ('). Spatial data refer to Cartesian coordinates. Since movements are mostly directed along the z-axis, the z-axis and the z'-axis coincide. The time is so adjusted that  $z=0\equiv z'=0$  at t=t'=0, resulting in the relations x'=x, y'=y,  $z'=\gamma(z-u_St)$ , and  $t'=\gamma(t-u_St)$  with  $\gamma=1/\sqrt{1-u_S^2/c^2}$  and the relative speed of the rest frames  $u_S$ . Seen from SRF, the radius of the shell is given by  $R'(t')=R'_0+R'_v(t')$  with  $R'_v(t')=A_S\left(erf\left((t'+t_0)/\tau\right)-erf\left((t'+t_1)/\tau\right)\right)$ , and  $R'_0$ ,  $A_S$ ,  $t_0$ ,  $t_1$ , and t being constants. For the radial velocity follows  $u'_R(t')=2A_S\left(\exp\left(-(t'+t_0)^2/\tau^2\right)-\exp\left(-(t'+t_1)/\tau^2\right)\right)/(\tau\sqrt{\pi})$ . A cross-section of the shell in a plane perpendicular to the z'-axis forms a circle with the radius  $r'(z',t')=\sqrt{R'(t')^2-z'^2}$  and seen from LRF r(z,t)=r'(z'(z,t),t'(z,t)).

With reference to SRF, the charge density is  $\sigma'_e(t') = Q/(4\pi R'(t')^2)$  with the total charge Q. With a shell of constant radius  $(A_s = 0)$ , the charge density as seen from LRF is  $\sigma_e(z) = Q\sqrt{\cos^2(\vartheta) + (\sin(\vartheta)/\gamma)^2}/(4\pi R_0^2)$  with  $\vartheta = \cos^{-1}(\gamma z/R_0)$  denoting the elevation angle with respect to the z-axis. If the incident radiation is independent of the y-coordinate, the z-component of the electric field acting on the charge at the plane defined by  $z = \zeta$  when the center of the shell is at (x, z, t) is given by

$$E_{\zeta}(x,z,\zeta,t) = \int_{0}^{2\pi} \text{Re}\left(E_{z}\left(x + R_{0}\sqrt{1 - (\gamma(z - \zeta)/R_{0})^{2}}\cos\varphi,\zeta,t\right)d\varphi\right).$$
 The total force acting in z - direction on the shell is obtained by integrating over the z-axis:

$$F_{z}\left(x,z,t\right) = R_{0} \int_{z-\frac{R_{0}}{\gamma}}^{z+\frac{R_{0}}{\gamma}} E_{\zeta}\left(x,z,\zeta,t\right) \sigma_{e}\left(\zeta\right) \sqrt{1-R_{0}\left(\gamma^{4}-\gamma^{2}\right)\zeta^{2}} \ d\zeta.$$

If the radius of the shell is time-dependent, the charge density is not only affected by relativistic length contraction but also by the deformation of the shell due to the dependence of the phase of the radial oscillation on the z-coordinate, as seen from LRF. In order to avoid computing the charge density explicitly, the forces are obtained by integrating the charge density belonging to R' instead of R over  $\vartheta'$  but multiplying with the incident field at the position where the charge is seen from LRF. For a given value of  $\vartheta'$  the value of z with  $\vartheta'(z,t) = \cos^{-1}(z'(z,t)/R'(t'(z,t)))$  is numerically approximated. Then r(z,t),  $u'_R(t'(z,t))$ , and  $u_R = u'_R \sin \vartheta' / (\gamma(1+u_S u'_R \cos(\vartheta')/c^2))$  can be determined. The forces acting on the charged circle defined by  $\vartheta'$  are integrated,

$$F_{CEz}(\vartheta',t) = \frac{Q r}{4\pi R'(t'(z,t))} \int_{0}^{2\pi} \text{Re}\left(E_{z}\left(x_{off} + r\cos\varphi, r\sin\varphi, z, t\right)\right) d\varphi \text{ and}$$

$$F_{CBz}(\vartheta',t) = \frac{Q r u_{R}}{4\pi R'(t'(z,t))} \int_{0}^{2\pi} \text{Re}\left(-B_{x}\left(x_{off} + r\cos\varphi, r\sin\varphi, z, t\right)\sin\varphi + B_{y}\left(x_{off} + r\cos\varphi, r\sin\varphi, z, t\right)\cos\varphi\right) d\varphi$$

(R' in the denominator in both  $F_{CEz}$  and  $F_{CBz}$  is not squared because otherwise it had to be multiplied in the integration over  $\vartheta'$ .) These forces are integrated over  $\vartheta'$ :

$$F_{Ez}(t) = \int_{0}^{\pi} F_{CEz}(\mathcal{S}, t) d\mathcal{S} \text{ and } F_{Bz}(t) = \int_{0}^{\pi} F_{CBz}(\mathcal{S}, t) d\mathcal{S}.$$

Please note that both sets of field equations comply with the Maxwell equations identically. The first set describes the inhomogeneous plane field:

$$x_{f} = x \cos \alpha - z \sin \alpha, \qquad z_{f} = x \sin \alpha + z \cos \alpha, \qquad E_{T} = A_{f} \cosh(\beta) e^{-\sinh(\beta)k x_{f}} e^{i(\omega t - \cosh(\beta)k z_{f} + \psi)},$$

$$E_{L} = -A_{f} \sinh(\beta) e^{-\sinh(\beta)k x_{f}} e^{i(\omega t - \cosh(\beta)k z_{f} + \psi)}, \qquad E_{x} = E_{T} \cos \alpha + E_{L} \sin \alpha, \qquad E_{y} = 0,$$

$$E_{z} = -E_{T} \sin \alpha + E_{L} \cos \alpha, \quad B_{x} = 0, \quad B_{y} = \frac{A_{f}}{C} e^{-\sinh(\beta)k x_{f}} e^{i(\omega t - \cosh(\beta)k z_{f} + \psi)}, \quad B_{z} = 0.$$

The equations of the radially polarized beam are obtained by a method following Mitri [8]. Deviating from Mitri's procedure, here the beam is limited to asymmetric components, resulting in  $H_z = 0$ . The field components are derived from a vector potential field with only a z-component

$$A_{z} = A_{0} \frac{zr}{2\sinh^{2}(kzr)} \left( \frac{\sin(kR^{-})}{R^{-}} e^{kzr} - \frac{\sin(kR^{+})}{R^{+}} e^{-kzr} \right) \text{ with } R^{\pm} = \sqrt{x^{2} + y^{2} + (z \pm izr)^{2}} \text{ , according }$$

to 
$$\mathbf{H} = \frac{1}{\mu} \nabla \times \mathbf{A}$$
 and  $\mathbf{E} = \frac{i}{\varepsilon \omega} \nabla \times \mathbf{H}$ . This results in  $E_x = \frac{i A_0 c^2 zr}{2 \omega \sinh^2(k zr)} e^{-i(\omega t + \psi)} f_{Ex}$ ,

$$E_{y} = \frac{i A_{0} c^{2} zr}{2 \omega \sinh^{2}(k zr)} e^{-i(\omega t + \psi)} f_{Ey}, E_{z} = \frac{i A_{0} c^{2} zr}{2 \omega \sinh^{2}(k zr)} e^{-k zr - i(\omega t + \psi)} f_{Ez},$$

$$H_x = \frac{A_0 zr}{2\mu \sinh^2(kzr)} e^{-i(\omega t + \psi)} f_{Hx}$$
, and  $H_y = \frac{A_0 zr}{2\mu \sinh^2(kzr)} e^{-i(\omega t + \psi)} f_{Hy}$  with

$$\begin{split} f_{Ex} &= -\frac{3e^{kzy} k x (z-izr) \cos(kR^-)}{(R^-)^4} + \frac{3e^{-kzr} k x (z+izr) \cos(kR^+)}{(R^+)^4} + \frac{3e^{kzr} k x (z-izr) \sin(kR^-)}{(R^-)^5} - \\ & \frac{e^{kzr} k^2 x (z-izr) \sin(kR^-)}{(R^-)^3} - \frac{3e^{-kzr} x (z+izr) \sin(kR^+)}{(R^+)^5} + \frac{e^{-kzr} k^2 x (z+izr) \sin(kR^+)}{(R^+)^3} \\ f_{Ey} &= -\frac{3e^{kzr} k y (z-izr) \cos(kR^-)}{(R^-)^4} + \frac{3e^{-kzr} k y (z+izr) \cos(kR^+)}{(R^+)^4} + \frac{3e^{kzr} k y (z-izr) \sin(kR^-)}{(R^-)^5} - \\ & \frac{e^{kzr} k^2 y (z-izr) \sin(kR^-)}{(R^-)^3} - \frac{3e^{-kzr} y (z+izr) \sin(kR^+)}{(R^+)^5} + \frac{e^{-kzr} k^2 y (z+izr) \sin(kR^+)}{(R^+)^3} \\ f_{Ez} &= \frac{e^{2kzr} k y (x^2+y^2-2(z-izr)^2) \cos(kR^-)}{(R^-)^4} - \frac{k(x^2+y^2-2(z+izr)^2) \cos(kR^+)}{(R^+)^4} - \frac{3e^{2kzr} x^2 \sin(kR^-)}{(R^-)^5} - \\ & \frac{3e^{2kzr} y^2 \sin(kR^-)}{(R^-)^5} + \frac{2e^{-2kzr} \sin(kR^-)}{(R^-)^3} + \frac{e^{2kzr} k^2 x^2 \sin(kR^-)}{(R^-)^3} + \frac{e^{2kzr} k^2 y^2 \sin(kR^-)}{(R^-)^3} + \\ & \frac{3x^2 \sin(kR^+)}{(R^+)^5} + \frac{3y^2 \sin(kR^+)}{(R^+)^5} - \frac{2\sin(kR^+)}{(R^+)^3} - \frac{k^2 x^2 \sin(kR^+)}{(R^+)^3} - \frac{k^2 y^2 \sin(kR^+)}{(R^+)^3} - \frac{k^2 y^2 \sin(kR^+)}{(R^+)^3} \\ & f_{hx} &= \frac{e^{kzr} k y \cos(kR^-)}{(R^-)^2} - \frac{e^{-kzr} k y \cos(kR^+)}{(R^+)^2} - \frac{e^{kzr} y \sin(kR^-)}{(R^-)^3} + \frac{e^{-kzr} y \sin(kR^-)}{(R^+)^3} \\ & f_{hy} &= \frac{e^{kzr} k x \cos(kR^-)}{(R^-)^2} - \frac{e^{-kzr} k x \cos(kR^+)}{(R^+)^2} - \frac{e^{kzr} x \sin(kR^-)}{(R^-)^3} + \frac{e^{-kzr} x \sin(kR^-)}{(R^+)^3} \\ & + \frac{e^{-kzr} x \sin(kR^-)}{(R^+)^3} + \frac{e^{-kzr} x \sin(kR^-)}{(R^+)^3} \\ & + \frac{e^{-kzr} x \sin(kR^-)}{(R^+)^3} + \frac{e^{-kzr} x \sin(kR^-)}{(R^+)^3} + \frac{e^{-kzr} x \sin(kR^-)}{(R^+)^3} \\ & + \frac{e^{-kzr} x \sin(kR^-)}{(R^+)^3} + \frac{e^{-kzr} x \sin(kR^-)}{(R^+)^3} + \frac{e^{-kzr} x \sin(kR^-)}{(R^+)^3} \\ & + \frac{e^{-kzr} x \sin(kR^-)}{(R^+)^3} + \frac{e^{-kzr} x \sin(kR^-)}{(R^+)^3} + \frac{e^{-kzr} x \sin(kR^-)}{(R^+)^3} \\ & + \frac{e^{-kzr} x \sin(kR^-)}{(R^+)^3} + \frac{e^{-kzr} x \sin(kR^-)}{(R^+)^3} + \frac{e^{-kzr} x \sin(kR^-)}{(R^+)^3} \\ & + \frac{e^{-kzr} x \sin(kR^-)}{(R^+)^3} + \frac{e^{-kzr} x \sin(kR^-)}{(R^+)^3} + \frac{e^{-kzr} x \sin(kR^-)}{(R^+)^3} \\ & + \frac{e^{-kzr} x \sin(kR^-)}{(R^+)^3} + \frac{e^{-kzr} x \sin(kR^-)}{(R^+)^3} + \frac{e^{-kzr} x \sin(kR^-)}{(R^+)^3} \\ & + \frac{e^{-kzr} x \sin(kR^-)}{(R^+)^3} + \frac{e^{$$

#### REFERENCES

- [1] J. J. Thomson, "A Suggestion as to the Structure of Light", Phil. Mag., S. 6, Vol. 48, pp. 737-746, October 1924
- [2] C. W. Oseen, "Über die Wechselwirkung zwischen zwei elektrischen Dipolen und über die Drehung der Polarisationsebene in Kristallen und Flüssigkeiten", Ann. d. Physik, Vol. 48, pp. 1-56, 1915
- [3] H. H. Skilling, Fundamentals of Electric Waves, 1st ed., John Wiley, 1942, p. 104
- [4] J. A. Stratton, Electromagnetic Theory, McGraw-Hill Book Company, 1941, pp. 568-569
- [5] Henning F. Harmuth, "Antennas and Waveguides for Nonsinusoidal Waves", Academic Press, 1984
- [6] Mohamed Said Sanad, "Ultra-wideband monopole large current radiator", US patent US 6,650,302 B2, filed Jul. 1, 2002
- [7] Henning F. Harmuth, "Response to a letter by J. R. Wait on Magnetic Dipole Currents", IEEE Transactions on Electromagnetic Compatibility, Vol. 34, No. 3, Aug. 1992
- [8] F. G. Mitri, "Quasi-Gaussian electromagnetic beams", Physical Review A 87, 035804, March 2013